JOURNAL OF GEOPHYSICAL RESEARCH, VOL. 107, NO. D18, 8139, doi:10.1029/2001JD900142, 2002

Solar actinic radiation (280–420 nm) in the cloud-free troposphere between ground and 12 km altitude: Measurements and model results

A. Hofzumahaus and A. Kraus[1]

Institut für Atmosphärische Chemie, Forschungszentrum Jülich (FZJ), Jülich, Germany

A. Kylling

Norwegian Institute for Air Research (NILU), Kjeller, Norway

C. S. Zerefos

Laboratory of Atmospheric Physics (LAP), Aristotle University of Thessaloniki, Thessaloniki, Greece

Received 18 October 2000; revised 21 January 2001; accepted 22 January 2001; published 14 September 2002

[1] Airborne measurements of the spectrally resolved actinic flux (280–420 nm) between the ground and 12 km altitude have been made using a new calibrated dual-channel spectroradiometer. The measurements were made as part of the Photochemical Activity and Ultraviolet Radiation/Altitude Dependence of the Tropospheric Ozone Photolysis (PAUR/ATOP) measurement campaign in Greece during June 1996. Flights were made over the Agean Sea under cloudless conditions for various aerosol loads and solar zenith angles. The spectral actinic flux measurements are compared with radiative transfer model simulations based on the multistream discrete ordinate radiative transfer (DISORT) algorithm. All input to the radiative transfer model was provided by independent measurements performed simultaneously on the nearby island of Agios Efstratios. For altitudes between 3000–12,000 m the agreement between the measurements and the model simulations is within ±5% for wavelengths larger than 310 nm and within ±10% at 295–310 nm. For the lowest flight altitude, 108 m, the model underestimates the measured actinic flux systematically by about 12%. This may be partly explained by uncertainties in the aerosol optical properties and the surface albedo. Flights on days with small and large amounts of aerosols showed that under otherwise identical conditions the actinic flux increased by up to 10% when the aerosol amount was larger. *Index Terms:* 0360 Atmospheric Composition and Structure: Transmission and scattering of radiation; 0305 Atmospheric Composition and Structure: Aerosols and particles (0345, 4801); 0394 Atmospheric Composition and Structure: Instruments and techniques; *Keywords:* actinic radiation; solar ultraviolet; vertical profiles; radiative transfer; troposphere; spectroradiometry

Citation: Hofzumahaus, A., A. Kraus, A. Kylling, and C. S. Zerefos, Solar actinic radiation (280–420 nm) in the cloud-free troposphere between ground and 12 km altitude: Measurements and model results, *J. Geophys. Res.*, *107*(D18), 8139, doi:10.1029/2001JD900142, 2002.

1. Introduction

[2] Photodissociation of molecules by solar ultraviolet (UV) radiation drives most atmospheric chemistry. In the troposphere, photolysis processes occur only at wavelengths greater than 290 nm because radiation at shorter wavelengths is entirely absorbed in the upper atmosphere by ozone and molecular oxygen. At longer wavelengths, dissociation is limited by the energy of the photons required to break molecular bonds. As a result, most tropospheric photolysis reactions are confined to the ultraviolet spectral region between 290 nm and 420 nm. Examples for important photodissociation processes in the troposphere are the photolysis of ozone ($\lambda < 340$ nm), formaldehyde ($\lambda < 360$ nm), hydrogen peroxide ($\lambda < 400$ nm), or nitrogen dioxide ($\lambda < 420$ nm). These and other photolytic reactions have a large influence on the abundance of hydroxyl radicals (OH) controlling the self-cleaning of the atmosphere, and on the photochemical production of tropospheric ozone [e.g., *Levy*, 1974; *Fishman and Crutzen*, 1978; *Logan et al.*, 1981; *Ehhalt*, 1999]. It is therefore mandatory that atmospheric photochemistry models use accurate photolysis rate coefficients as input parameters, in order to describe reliably the chemical composition of the atmosphere and its possible change due to anthropogenic perturbations [e.g., *Liu and Trainer*, 1988; *Madronich and Granier*, 1992; *Fuglestvedt et al.*, 1994; *Dickerson et al.*, 1997; *Olson et al.*, 1997; *Jonson et al.*, 2000].

[3] Atmospheric chemistry models usually rely on photolysis rate coefficients (photolysis frequencies, J values) that are derived from theoretically calculated spectra of the solar actinic flux:

$$J = \int \sigma(\lambda,T)\,\phi(\lambda,T)\,F(\lambda)\,d\lambda. \quad (1)$$

[1]Now at Grünenthal GmbH, Aachen, Germany.

0148-0227/02/2001JD900142

Here J is the photolysis frequency (s^{-1}) of a molecule that has a wavelength- and temperature-dependent absorption cross section σ (cm^2) and quantum yield Φ. The actinic flux F (cm^{-2} nm^{-1} s^{-1}) is the spherically integrated photon radiance L (cm^{-2} nm^{-1} s^{-1} sr^{-1}) over a solid angle Ω of 4π sr:

$$F(\lambda) = \int L(\Omega, \lambda)\, d\Omega. \quad (2)$$

It represents the radiation that a molecule receives from all directions in the atmosphere and includes the contribution of the direct solar beam and diffuse radiation scattered by atmospheric molecules, aerosols, clouds, and the Earth's surface.

[4] Different radiative transfer models have been developed for the simulation of the actinic flux in the atmosphere. Some are based on fast two-stream methods [e.g., *Isaksen et al.*, 1977; *Luther*, 1980; *Madronich*, 1987] that approximate the angular distribution of the radiance. Other models use more sophisticated multistream methods, like the discrete ordinate radiative transfer (DISORT) method [*Stamnes et al.*, 1988] that allows to calculate the actinic flux directly. Although such models are widely used in atmospheric chemistry, only few tests have been made directly against actinic flux measurements in the troposphere, where scattering of radiation plays an important role.

[5] Radiative transfer models for the UV and visible part of the spectrum have mostly been tested against ground-based radiometric measurements of broadband or spectrally resolved irradiance [e.g., *Wang and Lenoble*, 1994; *Zeng et al.*, 1994; *Forster et al.*, 1995; *Mayer et al.*, 1997; *Kylling et al.*, 1998; *van Weele et al.*, 2000]. However, irradiance is only related, but not the same as actinic flux. It represents the cosine-weighted integrated radiance and is nearly insensitive to radiation orginating close to the horizon. To the contrary, the actinic flux has equal sensitivity to radiation from all directions.

[6] Models have been tested against ground-based data of photolysis frequencies of ozone (O_3) and nitrogen-dioxide (NO_2), measured by chemical actinometers [*Bahe et al.*, 1979; *Dickerson et al.*, 1979; *Madronich et al.*, 1983; *Shetter et al.*, 1992, 1996; *Lantz et al.*, 1996] and radiometers [*Balis et al.*, 2002]. These studies were sensitive to the broadband integrated actinic flux as well as to the molecular data (σ and Φ) chosen in the model calculation of the J values.

[7] In summer 1998 the International Photolysis Frequency Measurement and Model Intercomparison (IPMMI) in Boulder, Colorado, offered the opportunity to test for the first time different radiative transfer models against spectrally resolved actinic-flux measurements at ground. Calculated actinic flux spectra by seventeen different models were compared with spectrally resolved measurements for clear-sky conditions. In general, the majority of the models agreed well with each other for solar zenith angles less than about 60° and with measurements of two of three spectroradiometers [*Bais and Madronich*, 2000].

[8] While radiation models are usually tested against surface measurements, they are often applied to calculate the radiation field throughout the atmosphere. As such, a model versus measurement comparison for various altitudes in the troposphere under well defined atmospheric conditions provides a crucial and essential test of a radiative transfer model. In the troposphere, airborne data have been measured to date for the broadband actinic flux (330–390 nm) [*Vila-Guerau de Arellano et al.*, 1994] on a tethered balloon, and photolysis frequencies of O_3 or NO_2 have been measured on aircraft by chemical actinometers [*Dickerson et al.*, 1982; *Kelley et al.*, 1995], broadband filter radiometers [*Junkermann*, 1994; *Volz-Thomas et al.*, 1996; *Pfister et al.*, 2000; *Früh et al.*, 2000], and spectroradiometers [*Shetter and Müller*, 1999; *Crawford et al.*, 1999]. Some of these studies have determined vertical profiles of photolysis frequencies or actinic flux for well defined conditions allowing an absolute comparison with radiative transfer models.

[9] *Vila-Guerau de Arellano et al.* [1994] measured the total actinic flux with a broadband photoelectric detector (330–390 nm) in the marine boundary layer up to 1000 m height and found good agreement between measurements and a multi layer delta-Eddington model for total overcast conditions. *Kelley et al.* [1995] measured $J(NO_2)$ at altitudes from 0.2 to 7.6 km for clear sky and 58° solar zenith angle. They used measured aerosol data as model input and found very good agreement (within 6%) with multistream model calculations. Similar results were obtained by *Volz-Thomas et al.* [1996], who measured a vertical profile of $J(NO_2)$ with calibrated filter radiometers up to 7.5 km altitude under clear-sky conditions for a solar zenith angle of 35°. They applied standard atmospheric parameters in their models and found good agreement (within 6%) with a multidirectional and a discrete ordinate model. *Shetter and Müller* [1999] determined photolysis frequencies of 11 molecules from measured actinic flux spectra over the Pacific Ocean between sea level and 11.9 km altitude. Their J values were obtained under mostly cloudy conditions and were used by *Crawford et al.* [1999] to assess the cloud effect on the photolysis frequencies of O_3 and NO_2. *Crawford et al.* [1999] compared the observations with results from a four-stream discrete ordinate radiative transfer (DISORT) model which was initialized with parameters from the 1976 U.S. Standard Atmosphere for clear-sky conditions. The ratios of the measured to modeled $J(NO_2)$ values were found to lie in the range between 0.9–1.0 for most of the time during the flights with the clearest skies. However, experimental $J(NO_2)$ data measured by filter radiometers on the same flights were systematically higher than the model and spectroradiometer measurements by 20–30%. This discrepancy could not be resolved from the available data. *Früh et al.* [2000] measured vertical profiles of $J(NO_2)$ by filter radiometers in a clear and cloudy sky at altitudes below 2.5 km. They used detailed in situ measurements of the microphysical aerosol and cloud properties as model input and found mostly good agreement (10%) with the results of a delta-four-stream and a 16-stream discrete ordinate model.

[10] The present work is new in several respects. We present the first measurements of the spectrally resolved actinic flux (4π sr) over the range of 280–420 nm and over the vertical extent of the troposphere (0.1–12 km). The measurements provide altitude profiles of the spectral actinic flux for well defined conditions in a cloud-free atmosphere over a homogenous sea surface. The measurements are compared to a multistream radiative transfer model based on the DISORT code. All input parameters needed are fixed by independent measurements. Accordingly, a rigorous test of a state-of-the-art radiative transfer model is achieved throughout the troposphere for the ultraviolet part of the spectrum that is most relevant for tropospheric chemistry models.

[11] The airborne measurements were performed with a scanning actinic-flux spectroradiometer that we have used otherwise for ground-based measurements of the downwelling actinic flux [*Müller et al.*, 1995; *Kraus and Hofzumahaus*, 1998; *Hofzumahaus et al.*, 1999; *Kraus et al.*, 2000]. In this work the instrument was modified to enable measurements of the 4π sr actinic flux by using two separate inlet optics for the upwelling and downwelling radiation. A similar concept has been devel-

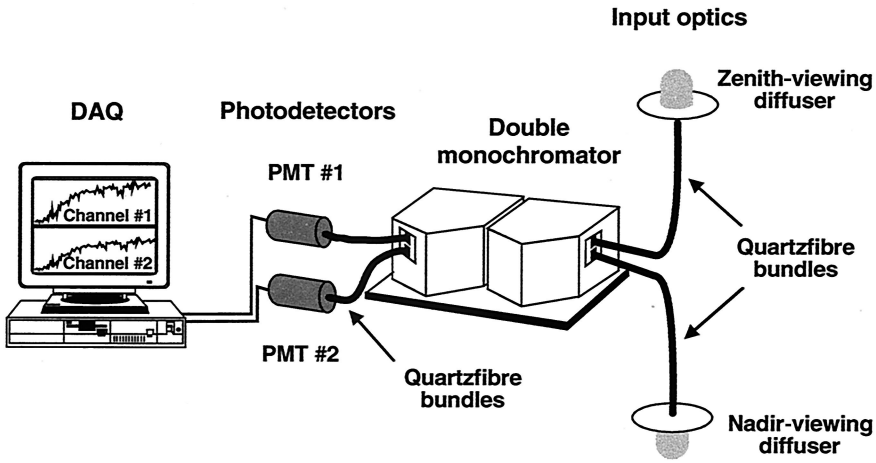

Figure 1. Schematic setup of the airborne dual channel actinic-flux spectroradiometer (DAQ, data acquisition system; PMT, photomultiplier tube). The zenith- and nadir-viewing inlet optics were mounted on top and at the bottom of the Falcon aircraft, respectively. The double monochromator, the photon detection system, and the data acquisition were installed inside the aircraft.

oped by *Shetter and Müller* [1999], who used two independent 2π sr spectroradiometers to measure the total 4π sr actinic flux.

[12] The measurements in this work were made in a joint field campaign in Greece in June 1996 within the frame of two European Union (EU) projects, Altitude Dependence of the Tropospheric Ozone Photolysis (ATOP) frequency between 0–12 km and Photochemical Activity and Ultraviolet Radiation (PAUR). Besides the airborne actinic flux measurements, ground-based measurements of spectral and broadband UV irradiances, aerosol optical depth and profile measurements, and total ozone column and ozone profile soundings have been taken at several places in the region of the Aegean Sea. The ground-based irradiance measurements and complementary modeling results were presented by *Kylling et al.* [1998]. Here the ground-based data are used to constrain the model input data for the simulation of the vertical radiation profiles, such that all model input parameters are from or based on analysis of independent measurements.

[13] The paper will first describe the modifications of the spectroradiometer system and its calibration. Next the various flights are described, and examples of measured spectra and their vertical distributions are provided. The radiative model and its input data are briefly presented, and a discussion follows of the comparison between the model simulations and the measurements. By comparing airborne measurements from 2 days with different aerosol loads, the influence of enhanced aerosol on the vertical actinic flux profiles is demonstrated.

2. Experiment

2.1. Spectroradiometer

[14] The spectroradiometer installed on board the Deutsche Luft-und Raumfahrt (DLR) Falcon-20E research aircraft was equipped with two measurement channels recording separately the upwelling and downwelling actinic flux. Each channel measured radiation from 280 to 420 nm with a spectral resolution (full width at half maximum) (FWHM) and step width of 1.0 nm. The spectroradiometer was a modified version of the ground-based instrument described in detail by *Hofzumahaus et al.* [1999]. Here we discuss only the modifications made to the airborne instrument.

[15] The main difference is the number of measurement channels. While the ground-based version used a single 2π sr inlet optic for the detection of radiation from one hemisphere, the aircraft instrument uses a combination of two receivers (2π sr) covering a total field of view of 4π sr (Figure 1). The upward pointing (zenith viewing) optic receives downwelling radiation from the Sun and the sky, while the downward pointing (nadir viewing) optic collects upwelling radiation that is backscattered by the underlying atmosphere and the ground.

2.2. Inlet Optics

[16] The inlet optics are quartz diffusers custom made by Meteorologie Consult GmbH (Glashütten, Germany) and are similarly constructed as the diffuser used for ground-based measurements [*Hofzumahaus et al.*, 1999]. Each optic is mounted in a pressure tight flange which carries an artificial horizon (80 mm diameter) limiting the field of view to one hemisphere. The zenith viewing optic was installed on top of the aircraft fuselage and the nadir viewing optic at the bottom. Both sensors were oriented with a slight tilt with respect to the fuselage in order to compensate the nick angle (typ. 5°) of the aircraft during the measurements at a constant altitude level. The angular sensitivity with respect to incident radiation was measured with a point light source for both sensors in the laboratory [cf. *Hofzumahaus et al.*, 1999] and adjusted to provide the best possible isotropy for the measurement of the 4π sr actinic flux. The resulting angular sensitivity is shown as a polar plot in Figure 2 for the zenith- and nadir-viewing diffusers (dotted and dashed lines, respectively) and for the combined optics (solid black line). The individual 2π sr receivers show a significant drop in sensitivity at polar angles above 70° and reach zero sensitivity at $\sim$ 110°. The combined 4π sr system shows good isotropy except near the horizon where the relative sensitivity is too high. In principle, the angular response can be improved by using an artificial horizon with a larger diameter [see *Volz-Thomas et al.*, 1996; *Shetter and Müller*, 1999]. In the present work this would have required an additional shadow ring mounted on top of the aircraft; however, such construction was not permitted for flight safety reasons.

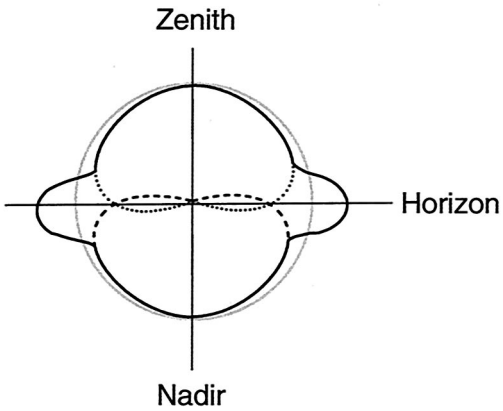

Figure 2. Polar diagram of the relative angular sensitivity of the inlet optic of the airborne spectroradiometer. The dotted and dashed lines represent the sensitivities of the zenith- and nadir-viewing optics, respectively; the solid line represents the sum of both optics. For comparison, the reponse of an ideal 4π sr system is shown (gray line).

2.3. Spectral Radiation Measurements

[17] The radiation collected by the input optics is transmitted via two quartz fibre bundles (Gigahertz Optik GmbH) to the entrance slit of the scanning double monochromator (BENTHAM DTM 300, 300 mm focal length, 2400 mm^{-1} gratings). In order to accomodate the incoming radiation from the zenith- and nadir-viewing diffusers separately, the entrance slit (20 mm height, 1.48 mm width) is divided vertically into three segments. The upper and lower segments (each 7 mm high) are open, while the middle part is masked (6 mm high). Each open segment is illuminated by one of the optical fibre bundles. Owing to the optical imaging properties of the monochromators, the entrance segments are imaged one-to-one onto the exit slit of the second monochromator. Here the radiation from the upper and lower exit slit is collected separately by two other quartz fibre bundles (Gigahertz Optik GmbH). These guide the photons to a pair of bialkali-photomultiplier detectors (EMI 9250QB), each connected with an amplifier and analog-to-digital converter electronics [*Hofzumahaus et al.*, 1999]. This setup constitutes two independent measurement channels that share the scanning double-monochromator and are therefore perfectly synchronized in measurement time and wavelength position. Calculation of the total (4π sr) actinic flux is easily accomplished by adding the measured spectra of the upwelling and downwelling radiation.

[18] The signal of each photodetector is associated almost exclusively with radiation from one of the inlet optics, except for a small contribution of light from the opposite receiver. The latter contribution is caused by imaging errors (astigmatism) of the monochromators, leading to a weak overlap of the entrance slit images with the opposite exit slit segments, causing an internal cross-talk of 5×10^{-4} between the two measurement channels.

2.4. Calibration and Accuracy

[19] The spectral sensitivity of the spectroradiometer was calibrated at the beginning and at the end of the campaign using certified irradiance standards (FEL 1000 W and 200 W tungsten-halogen quartz lamps) traceable to national standards laboratories (PTB, NIST) [*Hofzumahaus et al.*, 1999]. In addition, the calibration was checked at ground before and after each flight using portable secondary standards. The overall calibration error was about $\pm 6\%$ (2σ), and the detection limit was $\sim 10^9$ photons cm^{-2} nm^{-1} s^{-1}.

[20] The wavelength reading of the spectrometer was initially calibrated with an uncertainty of ± 0.02 nm against the emission lines of a low-pressure mercury lamp at ground. In addition, the wavelengths of the measured spectra were checked versus the positions of the Fraunhofer lines in the extraterrestrial solar spectrum (ATLAS 3, M. E. VanHoosier, personal communication 1996). Good agreement for the wavelength positions was found within ± 0.05 nm at ground and on the lowest flight levels up to an altitude of 6 km. Above that height the Fraunhofer-line analysis revealed an offset of the wavelength readings that increased with altitude from 0.4 nm at 9 km to 0.7 nm at 12 km. The wavelengths of the spectra shown in this work have been corrected for this effect.

[21] It is interesting to note that the observed wavelength shift was constant on each flight level at which typically 4–5 spectra were recorded sequentially. Moreover, its altitude dependence was reproducible from flight to flight, i.e., from day to day. No reason has been discovered that can explain the observed behavior. In particular, it cannot be explained by an influence of temperature and pressure on the spectroradiometer, as both parameters were stable to within a few percent inside the aircraft during the flights.

[22] Besides the calibration of the spectroradiometer, the imperfect isotropy of the angular response of the input optics causes an error. The individual 2π sr receivers underestimate the hemispheric actinic flux at polar angles up to 90°, but receive a contribution from the opposite hemisphere near the horizon. For the 4π actinic flux these systematic errors compensate each other partially. In the model section below it is shown that the remaining error causes an overestimation of the total actinic flux by at most 4% at all altitudes (0–12 km), if not corrected.

[23] In this context the error due to the internal cross-talk (5×10^{-4}) of the measurement channels inside the monochromators is negligible. If the upwelling and downwelling actinic fluxes differ by no more than a factor of 20, the error in any channel never exceeds 1%. During the campaign this condition was always fulfilled.

3. Measurements

[24] Vertical profiles of the 4π sr actinic flux were measured on board the DLR Falcon-20E aircraft on 4 days (10, 11, 13, and 14 June 1996) over Greece during the ATOP mission. In addition, in situ measurements of atmospheric ozone were made by a UV photometer, and water vapor, temperature, pressure, and geographical position were recorded by the aircraft standard equipment.

[25] One flight was performed on each measurement day. The flights had a duration of 2–3 hours and reached altitudes up to 12,200 m. The geographical position of the four flight tracks (F1–F4) is shown in Figure 3. The first three flights were carried out over the Aegean Sea close to the island Agios Efstratios (39.5°N, 24.5°E), and the fourth flight (F4) was carried out mostly over land surfaces near Athens (38.3°N, 23.8°E). At the same time, solar spectral irradiance measurements and soundings of atmospheric ozone and aerosol were performed in the frame of the PAUR project at three ground-based stations (Athens, Thessaloniki, and Agios Efstratios) [*Marenco et al.*, 1997; *Kylling et al.*, 1998].

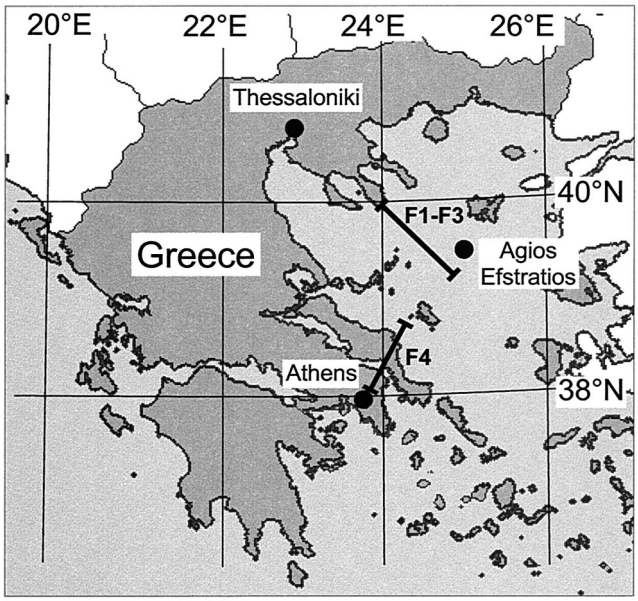

Figure 3. Map of Greece and the Aegean Sea. During the PAUR/ATOP campaign, ground-based measurements and soundings were performed at Athens, Thessaloniki, and on the island Agios Efstratios (solid circles). The positions of the four flight tracks (F1–F4) are indicated by the bars.

[26] During the flights over the Aegean Sea (F1–F3) the sky was cloud-free, whereas during the flight over land (F4) a few scattered clouds were present. The first flight (F1) was made around noon with solar zenith angles varying between 16.2°–24.5°. The aerosol load was relatively low with the total vertical aerosol depth τ(355 nm) = 0.28. The second flight was made for solar zenith angles between 32.1°–60.0° with slightly lower aerosol concentrations, τ(355 nm) = 0.21. During the third flight the aerosol load had increased, τ(355 nm) = 0.65, and the solar zenith angle was similar as on the first day, 16.1°–22.4°. The last flight was made over land near Athens for solar zenith angles between 16.1°–29.8° and τ(355 nm) = 0.8.

[27] Actinic flux measurements were performed at 5–6 constant altitude levels (100 m to 12,200 m) per flight during the aircraft ascent. At each level, 4–5 actinic flux spectra were measured successively for zenith and nadir view, each. The scan time per spectrum was 2.5 min. The spectra on each flight level had a good reproducibility (e.g., ±2% at 305 nm) and were averaged for each measurement channel. After wavelength correction, the averaged spectra of the upwelling and downwelling radiation were added to give the total 4π sr actinic flux. Examples of actinic UV spectra at different altitudes are shown in Figure 4. The data were recorded during the first flight (10 June 1996) and are plotted on a linear scale (left panel) for wavelengths between 290 and 420 nm. The sharply decreasing UV-B intensity below 310 nm is shown in a logarithmic plot in the right panel. For all UV wavelengths (290–420 nm) an increase in magnitude of the actinic flux can be noted toward higher altitudes. Obviously, the largest relative increase is found in the lowest 3 km, where most of the aerosol was located. The spectral range with the strongest altitude dependence is the UV-B, where atmospheric ozone absorbs solar radiation. The strong altitude dependence results in a pronounced shift of the UV-B edge toward shorter wavelength in the actinic spectra at higher altitudes (Figure 4, right panel). More data and discussion are presented below when the measurements are compared with model simulations. The measured data used in this study are available upon request (aircraft data from AH, ground-based data from CSZ).

4. Radiative Transfer Model

[28] The UVSPEC radiative transfer model was used to simulate the measured spectra. UVSPEC is part of the libRadtran package available from http://www.libradtran.org. The UVSPEC model includes various methods for solving the radiative transfer equation. Here the discrete ordinate radiative transfer equation solver of *Stamnes et al.* [1988] is used in 16-streams mode. A relatively large number of streams is needed since the actinic flux is calculated from the radiances output by the solver and the angular response of the instrument accounted for. Often the ideal actinic flux is calculated with two-streams approximation in order to save computer time. *Kylling et al.* [1995] showed that two-streams approximations under certain conditions may give errors of 20% compared to 16-streams calculations. The four-streams approximation is, however, sufficient for most calculations of the ideal actinic flux, yielding less than 1–2% error as sensitivity studies have shown in this work. To simulate a measured upwelling or downwelling actinic flux spectrum, azimuthally averaged radiances were calculated at 1° polar angle steps from nadir to zenith at high, 0.05 nm, spectral resolution. The resulting spectral radiances were convolved with the instrument slit function and interpolated to the center wavelength of the measurements. Finally, the radiances were multiplied with the angular response of the uplooking and downlooking input optics and integrated over the appropriate polar angle intervals to yield the simulated spectrum. Changes in the solar zenith angle due to changes in aircraft location and time duration of a single scan were accounted for. Temperature-dependent ozone cross sections were taken from *Bass and Paur* [1985], and the Rayleigh scattering cross section was calculated from the formula given by *Nicolet* [1984]. The extraterrestrial spectrum was taken from ATLAS 3 measurements (M. E. VanHoosier, personal communication, 1996) and shifted to air wavelengths. The Earth-Sun distance during the campaign was also accounted for. UVSPEC has been thoroughly compared against surface irradiance measurements [*Mayer et al.*, 1997; *Kylling et al.*, 1998; *van Weele et al.*, 2000].

[29] Input to the radiative transfer model are ozone profiles, aerosol optical depth, single scattering albedo and phase function profiles, and the surface albedo. Ozone profiles were taken from ozone sonde measurement made from the nearby airport of the city of Thessaloniki and are presented by *Kylling et al.* [1998, Figure 3]. The aerosol optical depth profiles were taken from simultaneous lidar measurements made on the nearby island of Agios Efstratios as described by *Marenco et al.* [1997]. The aerosol profiles were scaled to the total aerosol optical depth measured with a double Brewer spectroradiometer also located on Agios Efstratios and are presented by *Kylling et al.* [1998, Figure 4]. The aerosol single scattering albedo and phase function profiles and the surface albedo were taken as the values that provided the best agreement between model- and surface-based irradiance measurements by the Brewer spectroradiometer made simultaneously to the flight [*Kylling et al.*, 1998]. The main input parameters for the model simulations presented here are summarized in Table 1. All model input parameters are from or based on analysis of in-

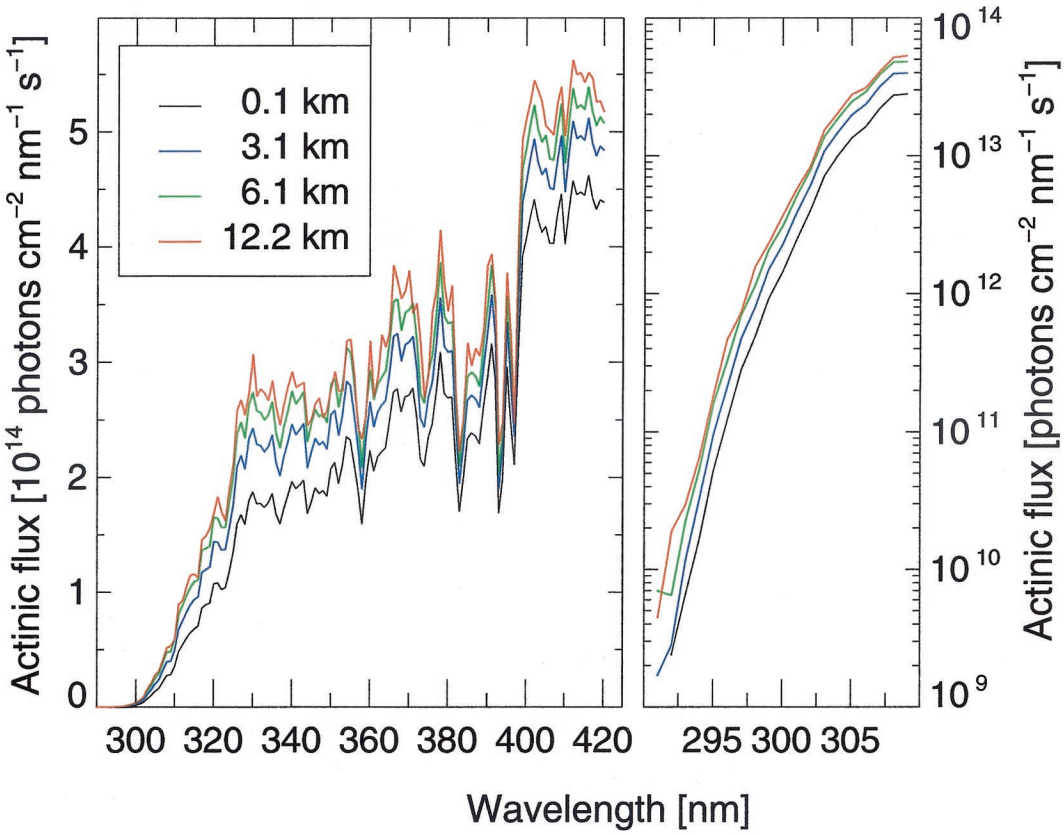

Figure 4. Spectra of the total actinic flux measured at different altitudes and cloud-free conditions over the Agean Sea on 10 June 1996. The solar zenith angle changed from 17° to 23° from the lowest to the highest flight level. Note the different scaling of the actinic flux in the left (linear) and right (logarithmic) panel.

dependent measurements. Thus the model/measurement comparison provides a precise test of our understanding of UV radiative transfer in the cloudless troposphere.

5. Comparison of Measurements and Simulations

5.1. Spectra

[30] Flights were performed on 4 days in June 1996 under varying atmospheric conditions as described above. As the model versus measurement results are similar for all days and flight levels, only results for the first flight on 10 June are presented in detail. The measured and simulated spectral actinic fluxes for five selected altitudes (122, 3045, 6094, 9141, and 12,189 m) are shown in the left column of Figure 5. Solid lines indicate the measurements and dashed lines the simulations. The corresponding model/measurement ratios of the actinic flux are plotted versus wavelength in the right column of Figure 5 (solid line). It should be noted that the model simulations take into account the measured angular response of the spectroradiometer input optics as explained in the previous section.

[31] Before we compare the measured and modeled spectra in detail, we first assess how closely the measurements and simulations approximate the ideal actinic flux. For this purpose, additional model runs have been performed for an ideal isotropic angular response. The ratio of the simulated to the ideal actinic flux is given by the dotted line in the right column of Figure 5. The deviations turn out to be small and vary only slowly with wavelength. They range from $\leq$1.4% at the lowest altitude to $\leq$3.6% at the highest flight level. The increasing deviations with altitude can be understood by the overlap of the angular response characteristics of the instrument (Figure 2) with the angular distribution of the diffuse radiance (Figure 6). The diffuse radiation field is more isotropic close to the surface than at 12 km. At 0.1 km most of the diffuse radiation is evenly distributed over the upper hemisphere. However, at high altitudes (e.g., 6.1 and 12.2 km) the largest contribution to the diffuse radiation field is from the horizon where also the

Table 1. Main Input Parameters to the Model Simulations for the 10 and 13 June Flights[a]

Parameter	10 June	13 June
Ozone Column, DU	342.6–344.7	330.3–334.6
Surface albedo	0.03	0.03
ω	0.87	0.95
g	0.70	0.70
α	1.04–0.683	1.22–0.72
β	0.091–0.138	0.17–0.31
τ (355 nm)	0.267–0.280	0.601–0.653

[a]Here ω is the aerosol single-scattering albedo, g is the aerosol asymmetry factor, α and β are the Ångström coefficients, and τ (355 nm) is the total vertical aerosol optical depth at 355 nm. For some parameters, variations were observed during the flight. The observed range of these parameters is given with the first α corresponding to the first β, etc.

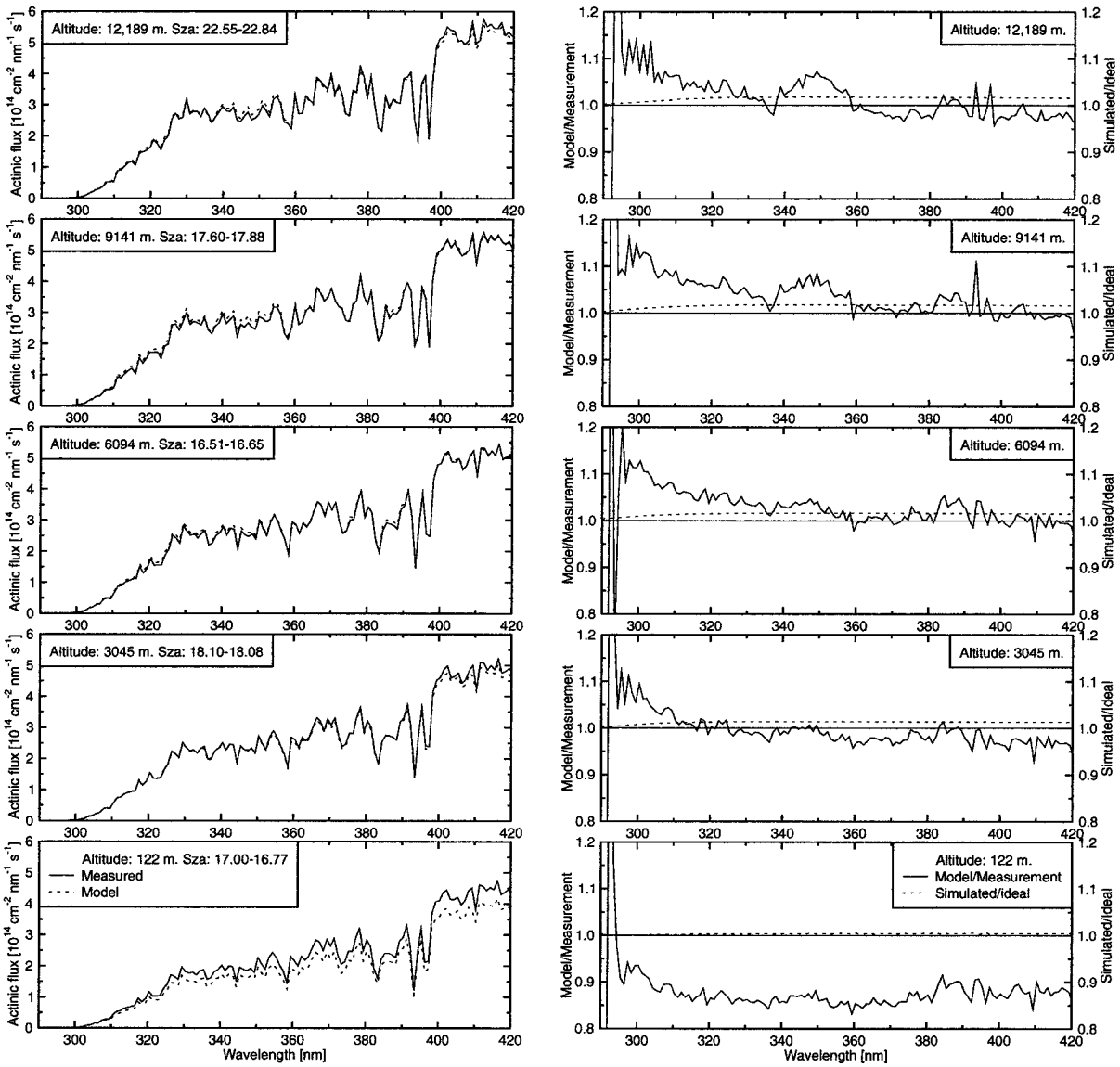

Figure 5. (left) Measured 4π actinic flux together with the simulated 4π actinic flux for selected altitudes. (right) Ratios of the measured and simulated actinic flux and the ratio of the simulated and ideal actinic flux. All data are from 10 June 1996.

angular response deviates most from a true 4π response. The relative contribution of direct radiation to the total acinic flux increases with height between 0.1 and 12 km: from 55% to 85% at 300 nm, from 55% to 70% at 330 nm, and from 70% to 77% at 400 nm. Thus a significant portion of the measured signal is direct radiation, which for the solar zenith angles encountered during these flights was minimally affected by the instrumental angular response. This explains the relative small differences

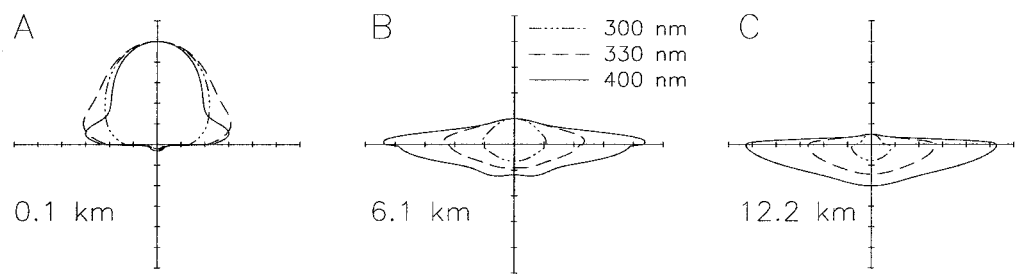

Figure 6. Relative angular distribution of the modeled diffuse radiance (azimuthally averaged and normalized to unity at the zenith) for the conditions of 10 June 1996. The radiance is shown for wavelengths of 300, 330, and 400 nm at altitude levels of (a) 0.1, (b) 6.1, and (c) 12.2 km.

between the simulated radiation and the ideal actinic flux. It may thus be concluded that for the conditions during these flights the measured actinic fluxes are at maximum 4% too high due to the nonideal 4π response of the input optics.

[32] The measured and simulated spectra agree very well with respect to their wavelength scales. This is not surprising as the measured spectra were calibrated versus the Fraunhofer line pattern in the ATLAS 3 spectrum which also served as input to the model. The good agreement therefore only demonstrates that the wavelength calibration of the experimental spectra has been performed properly. The absolute accuracy can be estimated from the comparison versus measurements of the mercury emission lines that have yielded agreement within ± 0.05 nm (see experimental section and *Hofzumahaus et al.* [1999]).

[33] The comparison of the absolute values of the measured and simulated actinic spectra shows generally good agreement at all altitudes. For wavelengths larger than 310 nm the differences between the model simulations and the measurements are within $\pm 5\%$, except for the lowest altitude where the model is about 12% systematically lower than the measurements. For wavelengths shorter than 310 nm the model/measurement ratio increases somewhat, reaching values of ~ 1.1 at 300 nm for 3–12 km altitude. Increasing the ozone column by about 1%, which is well within the experimental uncertainties of the ozone determination, removes this trend. Except for the lowest altitude, the differences are within the overall spectroradiometer error of $\pm 6\%$.

[34] The model-measurement discrepancy of 12% at the lowest flight level is not large, but significant with respect to the measurement uncertainty. One possible reason could be uncertainties in the model input data for the aerosols which were located below 3 km. Since the flights were not performed directly above the island of Agios Efstratios which was the site which provided the measurements for the model input parameters, there might be inaccuracies in the aerosol optical depth due to horizontal inhomogeneity. Decreasing the aerosol optical depth τ(355 nm) by 30% from 0.267 to 0.176 reduced the discrepancy only slightly from 12% to 9–10%. *Balis et al.* [2002] used an optical depth of 0.2 and an aerosol single scattering albedo of 0.96 for their simulations of the PAUR/ATOP actinic flux measurements. Repeating the simulations for the lowest layer with these input parameters left the model 7–8% lower than the measurements, similar to the results reported by *Balis et al.* [this issue, Figure 1]. Completely ignoring aerosols, which is unrealistic for the conditions during the campaign, left a 4–5% systematic difference between the model simulations and the measurements with the model being too low. Thus changing the aerosol optical properties could not bring the model results at the lowest altitude into an agreement with the measurement similar to the agreement found at higher altitudes.

[35] Another explanation for the discrepancy at the lowest level might be a too low value for the surface albedo. The value of 0.03 adopted for the simulations were taken as the value that provided the best agreement between model and surface based irradiance measurements by the Brewer spectroradiometer made simultaneously to the flight [*Kylling et al.*, 1998]. Slightly higher UV-albedo values have been reported in the literature. *Doda and Green* [1980] determined values of 0.05–0.08 from aircraft measurements over the ocean. *Blumthaler and Ambach* [1988] presented an experimental value of 0.05 for water. *Herman and Celarier* [1997] derived monthly climatological maps of the Earth's surface reflectivity from radiance measurements of the Nimbus 7/total ozone mapping spectroradiometer (TOMS). They report albedo values of 0.05–0.08 over the oceans. For the month of June a climatological mean value of 0.04–0.05 was found over the Aegean Sea [*Herman and Celarier*, 1997] (data available at ftp://jwocky.gsfc.nasa.gov/pub/surface_reflectivity). In order to test the sensitivity of the model results in this work to higher surface albedos, the value has been doubled from 0.03 to 0.06 leading to an increase of the actinic flux by $\sim 5\%$ at the lowest level and 2–3% at the highest level. This will slightly decrease the model-measurement difference. However, a clear distinction in the magnitude of the difference for the different altitudes is still present.

[36] The observed deviations between measurements and simulations in this work are similar to those reported by *Mayer et al.* [1997] for clear-sky UV irradiances at ground. They used the same radiative transfer model as in this work and compared the simulations with 1200 spectra measured in Garmisch-Partenkirchen, Germany. The systematic differences were between -11% and 2% for wavelengths between 295 and 400 nm.

[37] At longer wavelengths our results can be compared with studies of the NO_2 photolysis frequency by *Kelley et al.* [1995] and *Volz-Thomas et al.* [1996]. Both groups found good agreement within their experimental uncertainties of 6% between observed and modeled $J(NO_2)$ values under clear sky up to ~ 7.5 km altitude when they used multistream models for their simulations. Their results are consistent with our comparison at wavelengths around 370 nm, where the spectral distribution of the NO_2 photolysis frequency has its median.

5.2. Vertical Profiles

[38] The measured altitude dependence of the 4π sr actinic flux from 2 different days is presented for selected wavelengths in Figure 7 (upper panel). The solid lines connect data from the flight on 10 June when the aerosol load was relatively low. The dotted lines connect similar data for 13 June when the aerosol optical depth was larger by a factor of 2.4 at 355 nm. In both cases the sky was cloud-free, and the solar zenith angle was almost the same. A notable difference in the magnitude is observed between the vertical profiles of the 2 days, with higher actinic flux values at all wavelengths and altitudes when the aerosol load was higher.

[39] Model simulations were performed for 13 June in the same way as for 10 June. The atmospheric parameters used as model input are listed in Table 1. For 13 June a similar good agreement between the measured and simulated actinic flux was found as for 10 June. As a result, the simulated vertical profiles show a similar picture as the measured profiles (Figure 7, middle and lower panel).

[40] The vertical distribution of the actinic flux measured on 10 June, increases with altitude at all wavelengths. The largest relative change is observed across the lowest 3 km, where most of the backscattering aerosol was located [*Marenco et al.*, 1997; *Kylling et al.*, 1998]. The variation of the actinic flux with altitude depends strongly on wavelength. For example, the actinic radiation at 298 nm increases by about a factor of 3.3 between 0.1 and 12.2 km; this factor is reduced to 1.8 at 305 nm and to about 1.2 at 420 nm. At short wavelengths the relative strong variation with altitude is primarily due to the attenuation of solar radiation by the overhead ozone column, which decreases with increasing height in the atmosphere. This

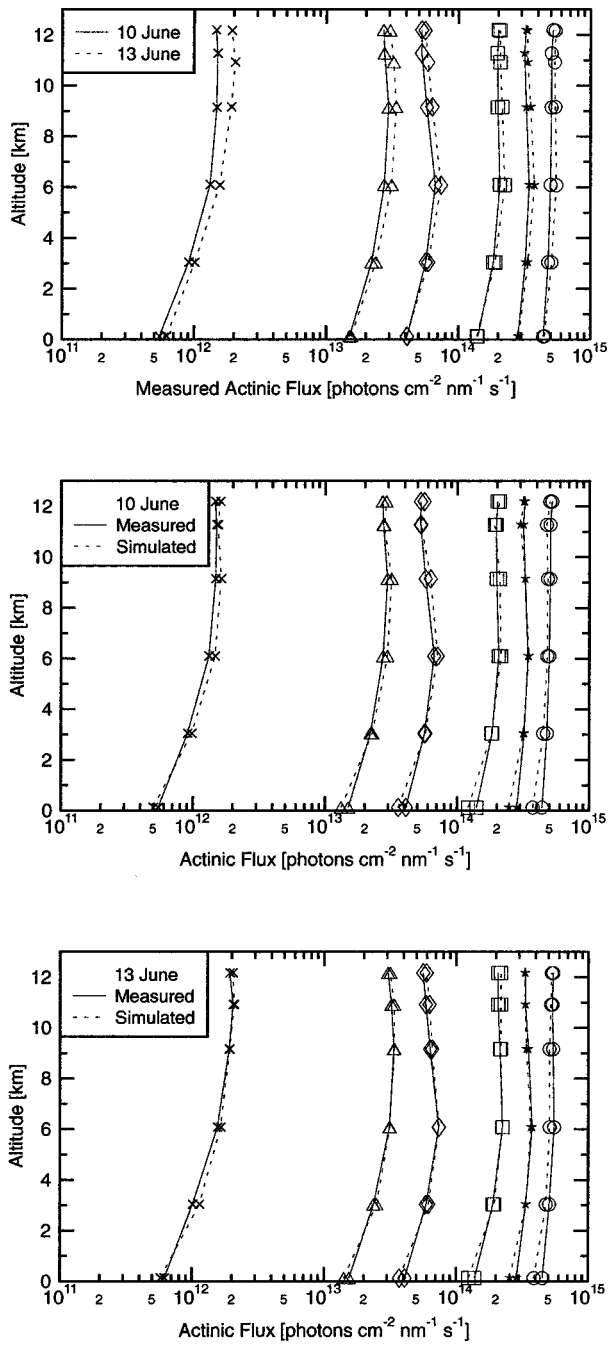

Figure 7. Measured and simulated altitude profiles of the total actinic flux over the Aegean Sea for selected wavelengths: crosses, 298 nm; triangles, 305 nm; diamonds, 310 nm; squares, 325 nm; stars, 380 nm; circles, 420 nm. (top) Measured actinic flux for 10 June (solid lines) and 13 June (dotted lines). (middle) Measured (solid line) and simulated (dotted lines) actinic fluxes for 10 June. (bottom) Similar to the middle plot, but for 13 June.

causes the UV-B edge of the actinic flux spectra to shift toward shorter wavelengths as seen in the right panel of Figure 4.

[41] The higher aerosol load on 13 June leads to a relative enhancement in the actinic flux above the aerosol layer due to increased backscattering. This is clearly seen in both the measured and simulated profiles. The actinic flux also increases slightly within the aerosol layer. The relative increase is largest for the shortest wavelengths; however, part of this is due to the ozone column being about 10 Dobson units (DU) lower on 13 June compared to 10 June. For wavelengths that are not affected by ozone absorption the higher aerosol amount leads to an increase in the actinic flux by up to 10%. The model simulation shows that this enhancement is due to the higher aerosol optical depth and the larger single-scattering albedo on 13 June (see Table 1). The source of the different aerosol has been explained by *Jonson et al.* [2000]. They report that sulfate aerosols were advected from Bulgaria to the island of Agios Efstratios. Sulfate aerosol has a single-scattering albedo near one which is close to the optical aerosol properties given in Table 1. On other occasions, Saharan dust has been observed to influence the solar UV over the Aegean Sea [*Balis et al.*, 2002]. Contrary to sulfate aerosol, Saharan dust is highly absorbing and has a single-scattering albedo closer to 0.77. If the increase in aerosol amount on 13 June 1996 had been due to Saharan dust, the actinic flux would have decreased.

6. Conclusions

[42] A new 4π actinic-flux spectroradiometer has been operated on board an aircraft during the joint PAUR/ATOP measurement campaign in Greece, June 1996. The instrument has provided the first actinic flux spectra in the troposphere at selected altitudes under well defined atmospheric conditions. The measurements extend over the spectral range of 280–420 nm and over altitudes between 0.1 and 12 km. The absolute calibration of the data is traceable to national standards and has an accuracy of 6%. Model simulations indicate that the deviations of the spectroradiometer inlet optic from the ideal 4π angular response resulted in a systematic measurement error of less than 3.6% for the conditions encountered during the campaign. Above 6 km a reproducible altitude-dependent wavelength shift has been observed in the measurements and was corrected against solar Fraunhofer lines. The wavelength accuracy of the final data is ± 0.05 nm.

[43] The actinic flux measurements were obtained under cloudless sky conditions for various solar zenith angles ($<60°$) and aerosol loads both over sea and land. The measurements were compared to a multistream radiative transfer model based on the DISORT method. All input to the model was fixed and derived from independent measurements and analysis. Moreover, the model simulations took into account the instrumental slit function and the angular response characteristics of the inlet optics. For altitudes between 3000–12,000 m the agreement between the measurements and the model simulations was within $\pm 5\%$ for wavelengths greater than 310 nm and within $\pm 10\%$ at 295–310 nm. At the lowest altitude the model was about 12% systematically lower than the observations. This discrepancy can only partly be explained by uncertainties in the aerosol amount and the surface albedo. In conclusion, the model-measurement comparison has constituted a rigorous test of the model since all model input was constrained by fixed, independent parameters. For the conditions of the campaign the test has demonstrated that the multistream method is an excellent tool to simulate accurately the ultraviolet actinic flux that is most relevant for photochemistry in the troposphere.

[44] Measurements and model simulations have provided consistently vertical profiles of the spectral actinic UV flux. At all wavelengths an increase with altitude was observed, with the strongest variation across the lowest 3 km and at wavelengths

in the UV-B spectral range. Comparison of measurements made on days with small and larger aerosol loads showed an increase in the actinic flux by up to 10% when the aerosol amount increased. These observations demonstrate the role of aerosol scattering and ozone absorption in the troposphere. The present data and the radiative transfer model will be used in future work to study in more detail the influence of scattering and absorption processes on photolysis frequencies in the troposphere.

[45] **Acknowledgments.** We would like to thank the participants of the PAUR project for logistical support during the joint field campaign, Wolfram Schrimpf for his help during the measurements, and the staff of the Falcon aircraft DLR-Oberpfaffenhofen for their assistance in preparing and performing the measurement flights. This work has been funded by the European Commission (contracts ENV4-CT95-0158 and ENV4-CT95-0048).

References

Bahe, F. C., W. N. Marx, U. Schurath, and E. P. Röth, Determination of the absolute photolysis rate of ozone by sunlight, $O_3 + h\nu \rightarrow O(^1D) + O_2(^1\Delta_g)$, at ground level, *Atmos. Environ., 13,* 1515–1522, 1979.

Bais, A. F., and S. Madronich, Evaluation of modeled and observed spectral actinic fluxes during the IPMMI campaign (abstract), *Eos Trans. AGU, 81*(19), Spring Meet. Suppl., A41E-02, 2000.

Balis, D. S., C. S. Zerefos, K. Kourtidis, A. F. Bais, A. Hofzumahaus, A. Kraus, R. Schmitt, M. Blumthaler, and G. P. Gobbi, Measurements and modeling of photolysis rates during the PAUR II campaign, *J. Geophys. Res., 107*(DX), 10.1029/2000JD000136, in press, 2002.

Bass, A. M., and R. J. Paur, The ultraviolet cross-section of ozone, I, The measurements, in *Atmospheric Ozone: Proceedings of the Quadrennial Ozone Symposium*, edited by C. S. Zerefos and A. Ghazi, pp. 606–601, D. Reidel, Norwell, Mass., 1985.

Blumthaler, M., and W. Ambach, Solar UVB-albedo of various surfaces, *Photochem. Photobiol., 48,* 85–88, 1988.

Crawford, J., D. Davis, G. Chen, R. Shetter, M. Müller, J. Barrick, and J. Olson, An assessment of cloud effects on photolysis rate coefficients: Comparison of experimental and theoretical values, *J. Geophys. Res., 104*, 5725–5734, 1999.

Dickerson, R. R., D. H. Stedman, W. L. Chameides, P. J. Crutzen, and J. Fishman, Actinometric measurements and theoretical calculations of $j(O_3)$, the rate of photolysis of ozone to $O(^1D)$, *Geophys. Res. Lett., 6*, 833–836, 1979.

Dickerson, R. R., D. H. Stedman, and A. C. Delany, Direct measurements of ozone and nitrogen dioxide photolysis rates in the troposphere, *J. Geophys. Res., 87*, 4933–4946, 1982.

Dickerson, R. R., S. Kondragunta, G. Stenchikov, K. L. Civerolo, B. G. Doddridge, and B. N. Holben, The impact of aerosols on solar ultraviolet radiation and photochemical smog, *Science, 278*, 827–830, 1997.

Doda, D. D., and A. E. S. Green, Surface reflectance measurements in the UV from an airborne platform, part 1, *Appl. Opt., 19*, 2140–2145, 1980.

Ehhalt, D. H., Photooxidation of trace gases in the troposphere, *Phys. Chem. Chem. Phys., 1*, 5401–5408, 1999.

Fishman, J., and P. J. Crutzen, The origin of ozone in the troposphere, *Nature, 274*, 855–858, 1978.

Forster, P. M. D. F., K. P. Shine and A. R. Webb, Modelling ultraviolet radiation at the Earth's surface, part II, Model and instrument comparison, *J. Appl. Meteorol., 34*, 2426–2439, 1995.

Früh, B., T. Trautmann, M. Wendisch, and A. Keil, Comparison of observed and simulated NO_2 photodissociation frequencies in a cloudless atmosphere and in continental boundary layer clouds, *J. Geophys. Res., 105*, 9843–9857, 2000.

Fuglestvedt, J. S., J. E. Jonson, and I. S. Isaksen, Effects of reductions in stratospheric ozone on tropospheric chemistry through changes in photolysis rates, *Tellus, Ser. B, 46*, 172–192, 1994.

Herman, J. R., and E. A. Celarier, Earth surface reflectivity climatology at 340-340 nm from TOMS data, *J. Geophys. Res., 102*, 28,003–28,011, 1997.

Hofzumahaus, A., A. Kraus, and M. Müller, Solar actinic flux spectroradiometry: A technique for measuring photolysis frequencies in the atmosphere, *Appl. Opt., 38*, 4443–4460, 1999.

Isaksen, I. S. A., K. H. Midtbo, J. Sunde, and P. J. Crutzen, A simplified method to include molecular scattering and reflection in calculations of photon fluxes and photodissociation rates, *Geophys. Norv., 31*, 11–26, 1977.

Jonson, J. E., A. Kylling, T. K. Berntsen, I. S. A. Isaksen, C. S. Zerefos and K. Kourtidis, Chemical effects of UV fluctuations inferred from total ozone and tropospheric aerosol variations, *J. Geophys. Res., 105*, 14,561–14,574, 2000.

Junkermann, W., Measurement of the $J(O^1D)$ actinic flux within and above stratiform clouds and above snow surfaces, *Geophys. Res. Lett., 21*, 793–796, 1994.

Kelley, P., R. R. Dickerson, W. T. Luke, and G. L. Kok, Rate of NO_2 photolysis from the surface to 7.6 km altitude in clear-sky and clouds, *Geophys. Res. Lett., 22*, 2621–2624, 1995.

Kraus, A., and A. Hofzumahaus, Field measurements of atmospheric photolysis frequencies for O_3, NO_2, HCHO, CH_3CHO, H_2O_2, and HONO by UV spectroradiometry, *J. Atmos. Chem., 31*, 161–180, 1998.

Kraus, A., F. Rohrer, and A. Hofzumahaus, Intercomparison of NO_2 photolysis frequency measurements by actinic flux spectroradiometry and chemical actinometry during JCOM97, *Geophys. Res. Lett., 27*, 1115–1118, 2000.

Kylling, A., K. Stamnes, and S.-C. Tsay, A reliable and efficient two-stream algorithm for spherical radiative transfer: documentation of accuracy in realistic layered media, *J. Atmos. Chem., 21*, 115–150, 1995.

Kylling, A., A. F. Bais, M. Blumthaler, J. Schreder, C. S. Zerefos, and E. Kosmidis, The effect of aerosols on solar UV irradiances during the photochemical activity and solar ultraviolet radiation campaign, *J. Geophys. Res., 103*, 26,051–26,060, 1998.

Lantz, K. O., R. E. Shetter, C. A. Cantrell, S. J. Flocke, J. G. Calvert, and S. Madronich, Theoretical, actinometric, and radiometric determinations of the photolysis rate coefficient of NO_2 during the Mauna Loa Observatory Photochemistry Experiment 2, *J. Geophys. Res., 101*, 14,613–14,630, 1996.

Levy, H., II, Photochemistry of the troposphere, *Adv. Photochem., 9*, 369–523, 1974.

Liu, S. C., and M. Trainer, Reponses of the tropospheric ozone and odd hydrogen radicals to column ozone changes, *J. Atmos. Chem., 6*, 221–233, 1988.

Logan, J. A., M. J. Prather, S. C. Wofsy, and M. B. McElroy, Tropospheric chemistry: A global perspective, *J. Geophys. Res., 86*, 7210–7254, 1981.

Luther, F. M., Annual report of Lawrence Livermore National Laboratory to the FAA on the high altitude pollution program: 1980, *Rep. UCRL-50042-80*, Lawrence Livermore Natl. Lab., Livermore, Calif., 1980.

Madronich, S., Photodissociation in the atmosphere, 1, Actinic flux and the effects of ground reflection and clouds, *J. Geophys. Res., 92*, 9740–9752, 1987.

Madronich, S., and C. Granier, Impact of recent total ozone changes on tropospheric ozone photodissociation, hydroxyl radicals, and methane trends, *Geophys. Res. Lett., 19*, 465–467, 1992.

Madronich, S., D. R. Hastie, B. A. Ridley, and H. I. Schiff, Measurement of the photodissociation coefficient of NO_2 in the atmosphere, I, Method and surface measurements, *J. Atmos. Chem., 1*, 3–25, 1983.

Marenco, F., V. Santacesaria, A. F. Bais, D. Balis, A. di Sarra, A. Papayannis, and C. Zerefos, Optical properties of tropospheric aerosols determined by lidar and spectrophotometric measurements (Photochemical Activity and Solar Ultraviolet Radiation campaign), *Appl. Opt., 36*, 6875–6886, 1997.

Mayer, B., G. Seckmeyer, and A. Kylling, Systematic long-term comparison of spectral UV measurements and UVSPEC modeling results, *J. Geophys. Res., 102*, 8755–8767, 1997.

Müller, M., A. Kraus, and A. Hofzumahaus, $O_3 \rightarrow O(^1D)$ photolysis frequencies determined from spectroradiometric measurements of solar actinic UV-radiation: Comparison with chemical actinometer measurements, *Geophys. Res. Lett., 22*, 679–682, 1995.

Nicolet, M., On the molecular scattering in the terrestrial atmosphere: An empirical formula for its calculation in the homosphere, *Planet. Space Sci., 32*, 1467–1468, 1984.

Olson, J., et al., Results from the Intergovernmental Panel on Climatic

Change Photochemical Model Intercomparison (PhotoComp), *J. Geophys. Res., 102*, 5979–5991, 1997.

Pfister, G., D. Baumgartner, R. Maderbacher, and E. Putz, Aircraft measurements of photolysis rate coefficients for ozone and nitrogen dioxide under cloudy conditions, *Atmos. Environ., 34*, 4019–4029, 2000.

Shetter, R. E., A. H. McDaniel, C. A. Cantrell, S. Madronich, and J. G. Calvert, Actinometer and Eppley radiometer measurements of the NO_2 photolysis rate coefficient during the Mauna Loa Observatory Photochemistry Experiment, *J. Geophys. Res., 97*, 10,349–10,359, 1992.

Shetter, R. E., C. A. Cantrell, K. O. Lantz, S. J. Flocke, J. J. Orlando, G. S. Tyndall, T. M. Gilpin, C. A. Fischer, S. Madronich, and J. G. Calvert, Actinometric and radiometric measurement and modeling of the photolysis rate coefficient of ozone to $O(^1D)$ during the Mauna Loa Observatory Photochemistry Experiment 2, *J. Geophys. Res., 101*, 14,631–14,641, 1996.

Shetter, R. E., and M. Müller, Photolysis frequency measurements using actinic flux spectroradiometry during the PEM-Tropics mission: Instrument description and some results, *J. Geophys. Res., 104*, 5647–5661, 1999.

Stamnes, K., S.-C. Tsay, W. Wiscombe, and K. Jayaweera, Numerically stable algorithm for discrete-ordinate-method radiative transfer in multiple scattering and emitting layered media, *Appl. Opt., 27*, 2502–2509, 1988.

van Weele, M., et al., From model intercomparison toward benchmark UV spectra for six real atmospheric cases, *J. Geophys. Res., 105*, 4915–4925, 2000.

Vila-Guerau de Arellano, J., P. G. Duynkerke, and M. van Weele, Tethered-balloon measurements of actinic flux in a cloud-capped marine boundary layer, *J. Geophys. Res., 99*, 3699–3705, 1994.

Volz-Thomas, A., A. Lerner, H.-W. Pätz, M. Schultz, D. S. McKenna, R. Schmitt, S. Madronich, and E. P. Röth, Airborne measurements of the photolysis frequency of NO_2, *J. Geophys. Res., 101*, 18,613–18,627, 1996.

Wang, P., and J. Lenoble, Comparison between measurements and modelling of UV-B irradiance for clear sky: A case study, *Appl. Opt., 33*, 3964–3971, 1994.

Zeng, J., R. McKenzie, K. Stamnes, M. Wineland, and J. Rosen, Measured UV spectra compared with discrete ordinate method simulations, *J. Geophys. Res., 99*, 23,019–23,030, 1994.

A. Hofzumahaus, Institut für Atmosphärische Chemie, Forschungszentrum Jülich, D-52425 Jülich, Germany. (a.hofzumahaus@fz-juelich.de)

A. Kraus, Grünenthal GmbH, D-52078 Aachen, Germany.

A. Kylling, Norwegian Institute for Air Research, P.O. Box 100, N-2027 Kjeller, Norway.

C. S. Zerefos, Laboratory of Atmospheric Physics, Aristotle University of Thessaloniki, GR-54006 Thessaloniki, Greece.